Methods and protocols in peripheral nerve regeneration experimental research: part II-morphological techniques

Methods and protocols in peripheral nerve regeneration experimental research. Part II – Morphological techniques

S. Raimondo, M. Fornaro, F. Di Scipio, G. Ronchi, M.G. Giacobini-Robecchi, S. Geuna.
Department of Clinical and Biological Sciences, San Luigi Gonzaga Medical School of the University of Turin, Italy
(From: *Int Rev Neurobiol.* 2009, 87,81-103)

Morphological techniqes for nerve research

Abstract

This paper critically overviews the main procedures used for carrying out morphological analysis of peripheral nerve fibers in light, confocal and electron microscopy. In particular, this paper emphasizes the importance of osmium tetroxide post-fixation as a useful procedure to be adopted independently from the embedding medium. In order to facilitate the use of any described techniques, all protocols are presented in full details. The pros and cons for each method are critically addressed and practical indications on the different imaging approaches are reported.

Moreover, the basic rules of morpho-quantitative stereological analysis of nerve fibers are described addressing the important concepts of design-based sampling and the disector. Finally, a comparison of stereological analysis on myelinated nerve fibers between paraffin- and resin-embedded rat radial nerves is reported showing that different embedding procedures might influence the distribution of size parameters.
***Keywords*:** Peripheral nerve fibers, Staining, Antibodies, Osmium tetroxide, Stereology

I. Introduction

Morphological analysis is the far most common method for the study of peripheral nerve regeneration (Vleggeert-Lankamp 2007; Castro et al., 2008). In fact, although in the clinical perspective functional assessment is the key element in the assessment of the nervous system, the investigation of nerve morphology can give us important information on various aspects of the regeneration processes (Hall, 2005; Geuna et al., 2009, this issue) which relates with nerve function (Kanaya et al. 1996).

The aim of this methodology-oriented paper is to describe the main morphological techniques for investigating the structure and ultrastructure of peripheral nerves with particular emphasis on the methods for the quantitative assessment of the morphological indicators of nerve function loss and recovery by design-based 2D stereology.

II. Light microscopy

II.1. Fixation procedures

Although different types of fixatives can be used for peripheral nerve histology, including Carnoy's fixative, Bouin's fluid fixation, we use 4% paraformaldehyde (Fluka, Buchs, Switzerland) in PBS (Phosphate Buffered Saline) for 2-4 h, followed by washing in 0.2 % glycine in PBS. To obtain good histological quality, perfusion is not required and it is enough to fix the nerve specimens by immersion in the fixative solution. During the first few seconds of fixation, the nerve segment has to be maintained straight in a small fixative drop in order to facilitate specimen's orientation and cutting.

II.2. Embedding procedures

The two most commonly embedding procedures for light microscopy are paraffin or cryo-embedding. The two techniques have both advantages and disadvantages and they can be alternatively chosen depending on the type of analysis that must be done.

Paraffin embedding provides a stronger support for the tissue and, in general, guaranties a better histology compared to cryo-embedding. On the other hand, the main limitation of paraffin is that antigenic sites are less exposed reducing the efficiency of an immunohistochemical analysis; moreover, the risk of tissue autofluorescence is higher. To overcome the latter limitation, prior to immunolabeling, sections can be processed with methods that facilitate antigen-antibody binding, including: a) three microwaves cycles of 5 minutes in EDTA solution (100mm); b) incubation in NH_4Cl for 10 minutes.

With cryo-embedding, tissue quality is less maintained compared to paraffin because the sudden change from liquid to solid phase of the tissue fluids. To overcome this problem, it is recommended to carry out sample cryo-protection with subsequent passages in increasing solutions of sucrose before the freezing step. The main advantage of cryo-embedding is that antigenic sites are less masked thus facilitating immunohistochemistry.

II.2.1. Paraffin embedding protocol

Specimens undergo a dehydration procedure in ethanol from 50% to 100%. Dehydration is followed by a diaphanization step in xylol or a substitute such as Bioclear (Bio-Optica, Milano, Italy).
Specimens are then maintained in liquid paraffin at 60°C over night (step 1) and then passed to a second passage in liquid paraffin at 60°C (step 2) before polimerization at room temperature.

Nerve sections are usually cut in a thickness range of 5-10 µm. Before staining, slides need to be deparaffinated and rehydrated with decreasing ethanol passages.

II.2.2. Cryo-embedding protocol

The specimens are rehydrated with PBS and cryo-protected with three passages in increasing solutions of sucrose (7.5% for 1 hr, 15% for 1hr, 30% over-night) in 0.1M PBS. Thereafter, specimens are maintained in a 1:1 solution of sucrose 30% and optimal cutting temperature medium (OCT) for 30 min and then embedded in 100% OCT. Specimens must then be store at –80°C.

Nerve sections are usually cut in a thickness range of 10-15 µm and must then be stored at –20°C. For staining, sections are taken out of freezer to room temperature and as soon as they are acclimatized, they can be further processed.

II.3. Staining procedures

II.3.1. Haematoxylin and eosin staining

Haematoxylin and eosin is the most commonly used stain for light microscopy observation in histology and histopathology. Haematoxylin labels nuclei in blue while eosin is detectable as a pink stain in cell cytoplasm. The slides are immersed in 0.1% haematoxylin (we use the product from Ciba, Basle, Switzerland) for 10 min, washed in tap water for 15 min, then immersed in 0.1% eosin (we use the product from Ciba, Basle, Switzerland) for 5 min and washed in distilled water. The sections are finally dehydrated in ethanol and mounted in DPX (we use the product from Fluka, Buchs, Switzerland).

Although very popular, it must be emphasized that haematoxylin and eosin is not an adequate method for nerve tissue staining because the myelin sheaths are not labeled and they are thus difficult to be detected (Fig. 1A).

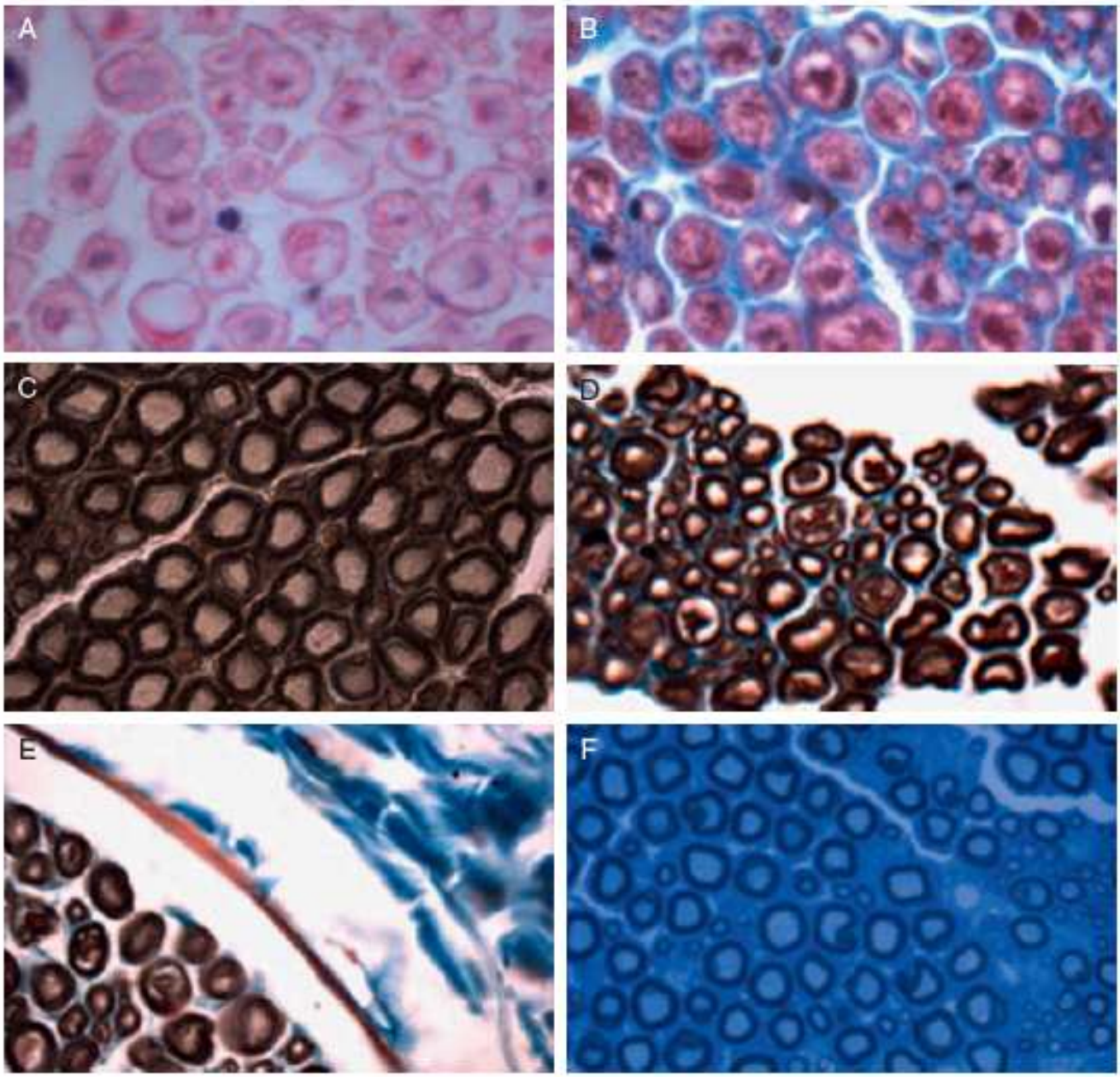

FIG. 1. High resolution light photomicrographs of cross sections of rat median nerve specimens processed by different methods. (A) Paraffin embedding and hematoxylin and eosin staining. (B) Paraffin embedding and Masson's trichrome staining. (C) Sections stained with osmium tetroxide before paraffin embedding. (D, E) Pre-embedding osmium tetroxide stained section counterstained with Masson's trichrome. (F) Resin embedding (with osmium tetroxide pre-embedding staining) and toludine blue staining. Magnification 600×.

II.3.2. Masson's trichrome staining

The quality of the histology of nerve sections stained with Masson's trichrome is higher compared to haematoxylin and eosin because it highlights also connective tissue. However, unless osmium tetroxide postfixation is carried out, myelin sheaths are not labeled with this method too (Fig. 1B).

For Masson's trichrome staining, in our laboratory we use a *Masson trichrome with aniline blue* kit (Bio-Optica, Milano, Italy): six drops of Weigert's iron haematoxylin (solution A) and six drops of Weigert's iron haematoxylin (solution B) are combined together and used to stain slides for 10 min. Without washing, the slides are then drained and incubated with ten drops of alcoholic picric acid

solution for 4 min. After washing in distilled water, sections are stained with ten drops of Ponceau acid fuchsin for 4 min and washed again in distilled water. Further on, ten drops of phosphomolybdic acid solution are added to the section for 10 min. Without washing, the slides are drained and 10 drops of aniline blue are added to the section for 5 min. Finally, after washing in distilled water, dehydrating rapidly in ethanol and clearing in xylol/Bioclear (Bio-Optica, Milano, Italy), the slides are mounted in DPX (Fluka, Buchs, Switzerland).

II.3.3. Pre-embedding myelin sheath stain with osmium tetroxide before paraffin embedding

The rationale for this procedure is to introduce osmium tetroxide's immersion prior to the embedding procedure also in case of paraffin embedding. This technique allows a better fixation of the myelin resulting in a better quality of the imaging. In fact, due to its action as a lipid fixative, post-fixation in osmium prevents myelin sheath swelling, which usually occurs during paraffin embedding, and provides the typical dark and sharp myelin stain, which greatly facilitates the identification of nerve fibers (Fig. 1C).

After fixation in 4% paraformaldehyde and washing in 0.2 % glycine in PBS for few minutes, specimens are immersed for 2 h in 2% osmium tetroxide (Sigma, St. Louis, MO) in Soerensen phosphate buffer (see IV.1). The nerves are then dehydrated in numerous passages in ethanol as described in the procedure for resin embedding (see IV.2) in order to completely remove excess of osmium from tissue. The specimens are then embedded in paraffin, cut and counter-stained with either haematoxylin and eosin or Masson's trichrome. Whereas myelin sheaths can be sharply detected right after applying the osmium post-fixation, (Fig. 1C), a very good histological quality can be obtained by Masson's trichrome counterstaining, which in particular allows a clear imaging of the nerve's connective structures (Fig. 1D,E).

II.3.4. Toluidine blue staining of semithin sections from resin-embedded blocks

The best quality for nerve analysis in light microscopy is obtainable after resin embedding (see IV.2) and toluidine blue staining (Fig. 1F). With this procedure, most of the myelinated axons can be clearly identified and myelin sheaths are sharply delimited due to lipid staining of osmium tetroxide post-fixation.

Semi-thin sections of nerve samples are usually cut in a thickness range of 1-3 µm with an ultramicrotome (we use a Ultracut UCT, Leica Microsystems, Wetzlar, Germany) and stained with 1% Toluidine blue (Fluka, Buchs, Switzerland) in 1% borax on a 80°C hot plate for 30-45 s.

II.3.5. Polychrome staining of semithin sections from resin-embedded blocks

This method serves the same purpose as the Toluidine blue procedure for staining semithin sections, but provides with red and blue colors (Hoffman et al. 1983). After stained with 1% Toluidine blue (Fluka, Buchs, Switzerland) in 1% borax on a 80°C hot plate for 30-45s, sections are incubated with a 1:1 solution of 0.1% basic fuchsin and in 1% borax on a 80°C hot plate for few seconds.

III. Immunohistochemistry and confocal microscopy

III.1. Fixation procedures

The most used fixation solution for immunohistochemistry and confocal microscopy is 4% paraformaldehyde as described for light microscopy (paragraph II.1). However, it is important to emphasize that since sample fixation can compromise immunolabelling by covering the antigenic sites, nerve segments intended for immunohistochemistry should be kept in fixative for 2-4 h depending on specimen's size.

III.2. Embedding procedures

For immunohistochemistry, tissue samples can be embedded in paraffin or ice as described above (paragraph II.2). Yet, the strategies for unmasking antigen sites can be applied as recommended in paragraph II.2. For nerve immunohistochemistry, we usually prefer embedding in paraffin. Cryo-embedding procedure must be used on GFP-autofluorescent samples since paraffin embedding, because of the ethanol passages, would delete GFP-autofluorescence.

III.2.1 “Etching” procedure for immunohistochemistry after pre-embedding osmium tetroxide staining

For immunohistochemistry and confocal laser microscopy on sections obtained from nerve specimens post-fixed in osmium tetroxide, the slides must be etched, after deparaffination, by incubating them in 3% H_2O_2 (Sigma, St.Louis, MO) for 10 min. This technique allows to use the same sample for both stereological and immunohistochemical analysis (Di Scipio et al., 2008).

III.3. Antibodies and immunostaining procedures

Both axon and glia can be detected by immunohistochemistry using specific antibodies. In particular, the most used antibodies as axon markers are those against neurofilament (NF) subunits. In our laboratory, we have used both anti-NF 200kda (monoclonal, mouse, Sigma, St.Louis, MO) and anti-PAN-NF (polyclonal, rabbit, Biomol). A-PAN-NF reacts with all three neurofilament proteins (68kda, 150kda and 200kda) and therefore it allows staining almost all myelinated nerve fibers. Figure 2 shows sciatic nerve of monkey (Fig 2A), rat (Fig 2B), mouse (Fig 2C), stained with NF-200kda. For mouse nerve tissue, a better result has been obtained using a-PAN-NF (Fig 2D).

Another useful axonal marker is anti-peripherin (polyclonal, rabbit, Chemicon, Billerica, MA, USA) that predominantly labels unmyelinated axons. Double labeling with anti-peripherin and anti-NF 200kd (Fig.3A,B), which predominantly labels myelinated axons, permits to distinguish between the two types of fibers (Fornaro et al., 2008). Other axonal markers that we commonly use are the anti-PGP 9.5 (polyclonal, rabbit, Biogenesis), that is found specifically in the PNS (Fig.2E), and anti-GAP43 (growth associated protein 43)(polyclonal, goat, Santa Cruz, Santa Cruz, USA) that is expressed at high levels during development and axonal regeneration. Finally, a marker selectively specific for motor axons is the anti-chat (choline acetyltransferase) (polyclonal, goat, Chemicon, Billerica, MA, USA) (Fig. 2G).

As far as Schwann cell recognition is concerned, they can be detected by immunohistochemistry using specific glial markers, such as GFAP and S100. Anti-GFAP antibody (in our lab we use both monoclonal, mouse, Dako, Denmark and polyclonal, rabbit, Sigma, St.Louis, MO) is the commonly used marker for immature and un-myelinating Schwann cells. Anti-S100 antibody (polyclonal, rabbit, Sigma, St.Louis, MO or Dako, Denmark) labels the cytoplasm and nucleus of Schwann's cells (Fig. 2F) and has been shown to be a very good marker of human peripheral nerves (Gonzalez-Martinez et al., 2003).

Glial markers can be associated with neuronal markers in double immuno-staining providing useful information on the relationship between axons and glial cells (Fig. 3C).

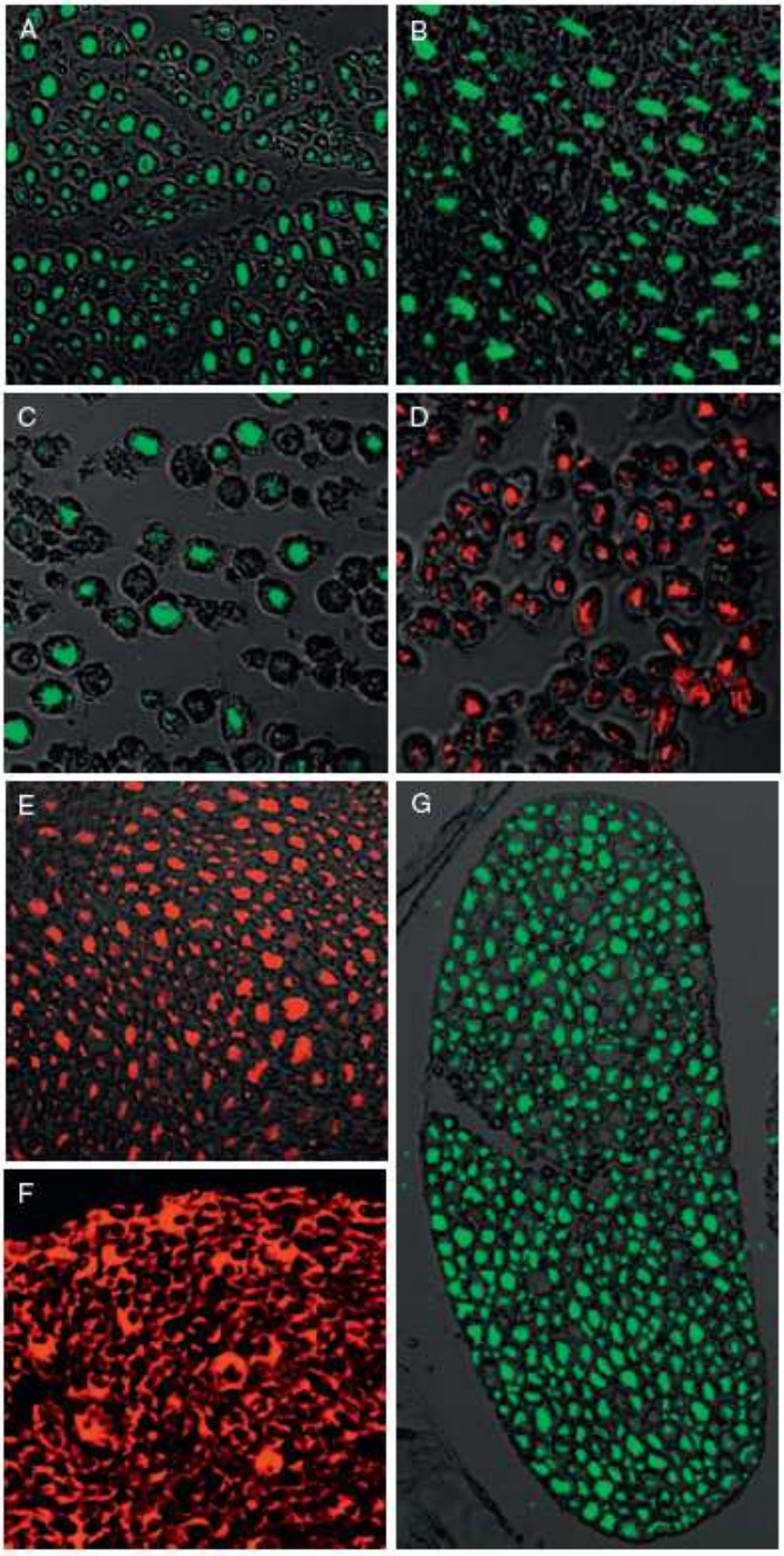

FIG. 2. Confocal images of different animal species normal nerves. (A–C) Immuno-staining with anti-NF 200 kDa of monkey (A), rat (B), and mouse (C) sciatic nerve. (D) Immuno-staining with

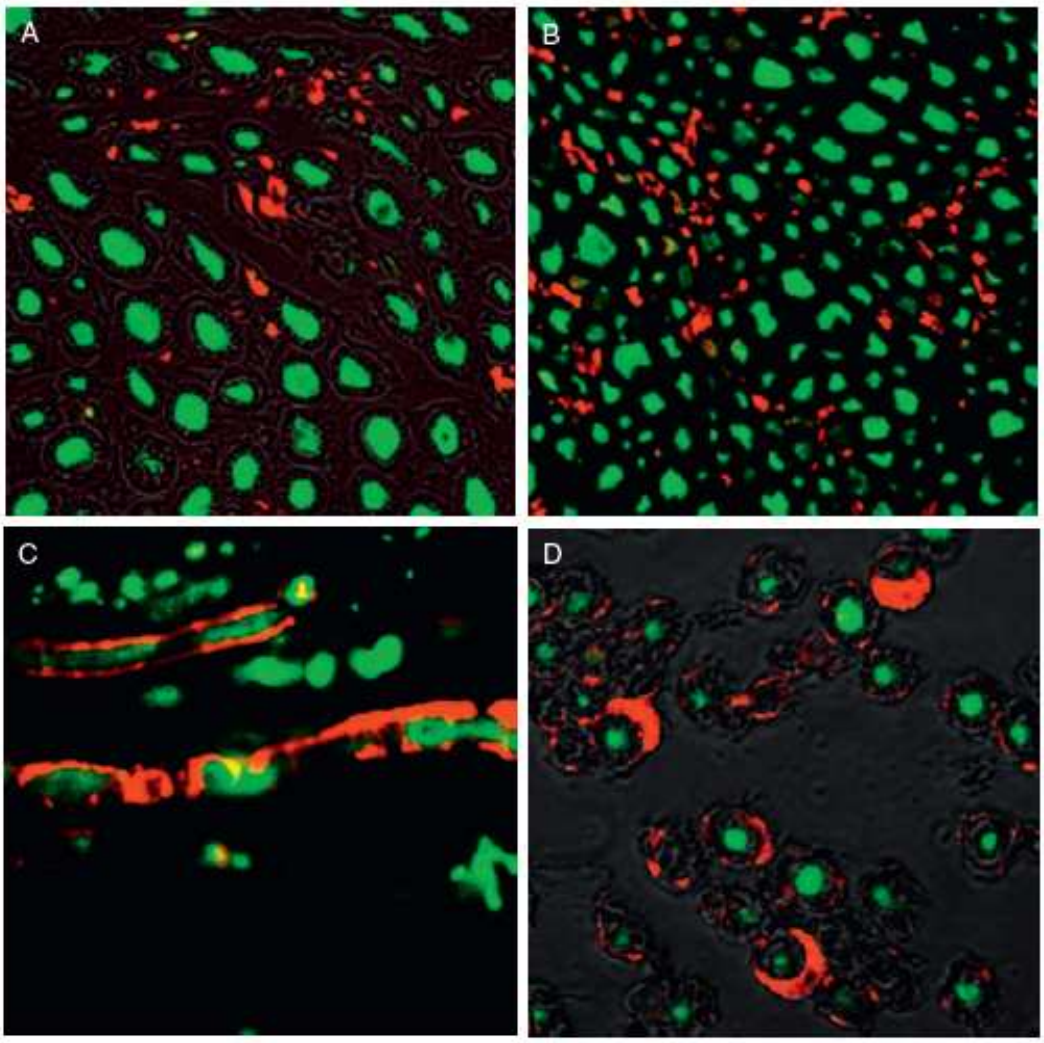

FIG. 3. Confocal images of monkey normal nerve (A) and rat normal sciatic nerve (B) double labeled with anti-NF 200 kDa and anti-peripherin. (C). Regenerating rat fibers double stained with anti-NF 200 kDa and S100. (D). Mouse median nerve double stained with anti-NF 200 kDa and erbB2. Magnifications: A–C = 600×; D = 1000×.

Beside their use as markers of different axons and glia, immunohistochemical analysis is also a useful tool to investigate cell function and molecular activity, for example the cellular signaling pathways. Particularly interesting for nerve regeneration is the NRG/erbb pathway system (Audisio et al., 2008; Casha et al., 2008). In several experimental studies we specifically focused on erbb2 expression in Schwann cells, testing different antibodies. The best results were obtained with the polyclonal antibody from Genetex (Fig. 3D).

III.3.1. Immunofluorescence

For immunofluorescence, the sections are rinsed in PBS, blocked with normal serum (1%), (the use of a normal serum made in the same species of the secondary antibody is recommended), for 1 h and then incubated overnight with the primary antibody. For double labelling, different primary antibodies can be used contemporarily as long as they are made in different animal species. If both antibodies are made in the same species, an “unconjugate affinity Fab fragment igg” protocol (Jackson Immunoresearch Laboratories, Baltimore, MD, USA) can be use (Fornaro et al., 2003). After primary antibody(ies) incubation, sections are washed three times in PBS and incubated for 1h in a solution containing the secondary antibody(ies) conjugated with a fluorofore and selected in order to recognize the species of primary antibodies. After three washes in PBS, sections are finally mounted with a Dako fluorescent mounting medium and stored at 4°C before being analyzed.

III.3.2. Immunoperoxidase

For immunoperoxidase staining the sections are rinsed in PBS and the endogenous peroxidase are inhibited with an incubation of 10 minutes in a solution of methanol (50%) and H_2O_2 (1%) in PBS. Sections are then blocked with normal serum (1%), made in the same species of the secondary antibody, for 1 hr and then incubated overnight with a primary antibody. The sections are washed three times in PBS and incubated for 1h in a solution containing a biotinylated secondary antibody against the same specie of the primary antibody. After three washes in PBS samples are then processed with peroxidase-conjugated Vectastain ABC kit (Vector, Burlingame, CA, USA) and revealed with diaminobenzidine (Sigma, St. Louis, MO). For double immuno-staining, the two immuno-labelling must be carried out separately and revealed using different enzyme-systems, such as peroxidase/phosfatase. The peroxidase protocol can also be used as a pre-embedding stain technique for electron microscopy immunolabelling.

IV. Electron microscopy

IV.1. Fixation procedures

We fix nerve samples in a solution of 2.5% purified glutaraldehyde (Histo-line Laboratories s.r.l., Milano, Italy) and 0.5% saccarose (Merck, Darmstadt, Germany) in 0.1M Sörensen phosphate buffer, ph 7.4, for 6-8h, then wash and store them in 0.1M Sörensen phosphate buffer added with 1.5% saccarose at 4-6°C prior to embedding (in our experience the nerves can be stored for several days or even weeks in buffer at 4-6°C with no problem). During the first few seconds of fixation, the nerve segment has to be maintained straight in a small fixative drop in order to facilitate specimen's orientation and cutting.

Sörensen phosphate buffer is made with 56g di-potassium hydrogen phosphate 3-hydrate (K_2HPO_4-$3H_2O$) (Fluka, Buchs, Switzerland) and 10.6 g sodium di-hydrogen phosphate 1-hydrate (nah_2po_4-H_2O) (Merck, Darmstadt, Germany) in 1 litre of doubly-distilled water.

Just before the embedding, nerves are washed for few minutes in the storage solution and then immersed for 2 h in 2% osmium tetroxide (Sigma, St.Louis, MO) in the same buffer solution.

IV.2. Embedding procedures

The specimens are carefully dehydrated in passages in ethanol from 30% to 100% with at least five passages of 5 min each. After two passages of 7 min each in propylene oxide (Sigma, St.Louis, MO) and 2h in a 1:1 mixture of propylene oxide and Glauerts' mixture of resins, specimens are embedded in Glauerts' mixture of resins, which is made of equal parts of Araldite M and the Araldite Härter, HY 964 (Merck, Darmstad, Germany). At the resin mixture, 2% of accelerator 964, DY 064 is added (Merck, Darmstad, Germany). For the final step a plasticizer (0.5% of dibutylphthalate) is added to the resin in order to promote the polymerization of the embedding mixture.

IV.3. Cutting and staining procedures

In our laboratory, thin sections of nerve samples are usually cut in a thickness range of 50-70 nm with an ultramicrotome (we use a Ultracut UCT, Leica Microsystems, Wetzlar, Germany). Sections are collected and placed on grids previously coated with pioloform film. For transmission electron microscope, grids are usually stained with uranyl acetate (sature solution) for 15 minutes and lead citrate for 7 minutes, washed and dried. As alternative to uranyl acetate it's possible to use Platinum blue (Inaga et al. 2007).

In the nerve, transmission electron microscopy analysis allows to investigate various ultrastructural features, including the organization of unmyelinated (Fig.4A) and myelinated (Fig. 4B) axons. Figure 4C shows a typical artifact of myelin sheaths, namely small swelling areas (arrow), that is commonly detected in peripheral nerves and that can be misinterpreted as a pathological sign.

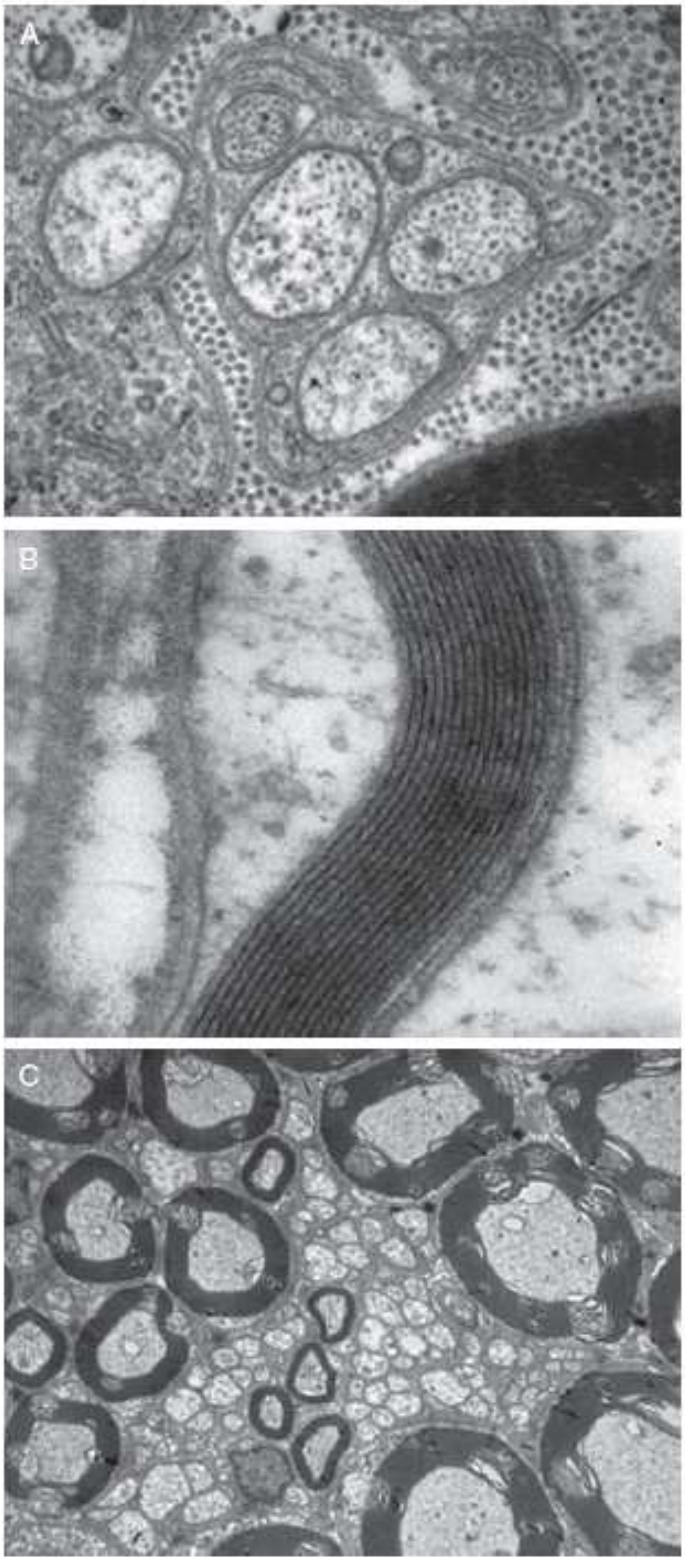

FIG. 4. Electron micrographs of nerve fibers. (A) Unmyelinated nerve fibers. (B) High magnification of a myelinated sheath. (C) Myelin sheath swelling, a typical artifact in large myelinated nerve fibers. Magnifications: A = 80,000×; B = 150,000×; C = 5000×.

V. Histomorphometry (stereology)

Quantitative estimation of nerve fiber morphology (especially myelinated ones) is, together with functional assessment, a key investigation tool in nerve regeneration research (Kanaya et al. 1996; Geuna et al., 2004; Vleggeert-Lankamp, 2007). The most important geometrical parameters that can be used for the assessment nerve fibers are: (1) Number of fibers, (2) Density of fibers, (3) Diameter of fibers and axons (Maximum, Minimum, Circle-equivalent), (4) Cross-sectional area of fibers and axons, (5) Perimeter of fibers and axons, (6) Myelin thickness, (7) Myelin-thickness/axon-diameter ratio, (8) Fiber-diameter/axon-diameter ratio or axon-diameter/fiber-diameter (g-ratio)

Although number and density of nerve fibers are the most used indicators of nerve regeneration, both parameters need to be carefully interpreted. In fact, a high number of regenerated nerve fibers can not only indicate a good regeneration, but also aberrant sprouting (in this case the contemporary assessment of fiber size can provide additional information). Data on fiber density are even more difficult to be interpreted since a high fiber density not always reflects good nerve regeneration, but can also reflect the presence of small regenerated axons. On the other hand, a low fiber density can reflect both large axons (that is a good predictor) and also the presence of oedema in the regenerated nerve (that is a bad predictor). Again in this case, the contemporary assessment of fiber size can facilitate interpretation of number and density data.

Fiber and axon diameter are the classical parameter for nerve type identification since they have proved to be the main determinant of conduction velocity (Hoffman, 1995). Various types of diameters of nerve fibers and/or axons can be used to assess their size (Geuna et al., 2001): the maximum diameter (which is strongly biased by obliquity of cross-sectional fiber profiles), the minimum diameter (which is strongly biased by fiber shrinkage), and the circle-equivalent diameter (which represents the diameter of a circle the area of which corresponds to the cross-sectional area of the fiber and/or axon). Cross-sectional area is another commonly used size estimation parameter for myelinated nerve fibers that, however, is not easy to be interpreted by readers since the diameter is classical parameter used to classify nerve fibers (Hoffman, 1995; Geuna et al., 2001).

Starting from rough data on the diameter of the fiber (D) and the axon (d), several other size parameters can be calculated by simple mathematical formulas: myelin thickness [(D-d)/2], the myelin-thickness/axon-diameter ratio [(D-d)/2d], the fiber-diameter/axon-diameter ratio (d/D), and its opposite the axon-diameter/fiber-diameter ratio, also called *g-ratio* (D/d).

These additional parameters are particularly important for the investigation of nerve development (Fraher et al., 1990) as well as nerve regeneration since they better correlate with the functional outcome of nerve recovery (Kanaya et al., 1996). Since quantification of size parameters is not always easy from a technical viewpoint, the selection of the indicators to be used in a given nerve regeneration study should be also done on the basis of the quality of the histological material and the equipment available.

The quantitative assessment of tissue and organs on histological sections has been the subject of heated scientific debate over the last years. In particular, the emergence of an new approach to cope with bias in morphometrical analysis, namely *stereology*, has represented a significant advancement in neuromorphology (for literature revision see: Coggeshall, 1992; Mayhew and Gundersen, 1996; West, 1999; Reed and Howard, 1998; Geuna, 2000, 2005; Benes and Lange, 2001; Guillery, 2002; von Bartheld, 2002; Schmitz and Hof, 2005; Baryshnikova et al., 2006; Canan et al., 2008).

Independently, of the parameters under investigation, there are at least five different sources of bias in the quantitative assessment of nerve fibers (Geuna et al., 2001). First, the strain, gender and age of experimental animals (strain-related, gender-related, age-related foundations of bias). Second, the point (level) along the nerve axis where sections are cut (section-related foundations of bias). Third, the location of the sampling fields within the nerve cross-section profile (location-related foundations of bias). Fourth, the inclusion-exclusion rules for sampling fiber profiles within the sampling fields (morphology-related foundations of bias). Fifth, the method for measuring the selected size parameters (measurement-related foundations bias). The first two potential sources of bias are related to the study

design. The other three sources are related to the sampling procedure and the method used for quantitative nerve fiber assessment and will thus be treated in this paragraph focusing, in particular, the basic principles and methods for design-based sampling and for nerve fiber stereology.

The ‘‘golden rule’’ of sampling for any tissue and organ is the equal opportunity rule (Cruz-Orive and Weibel, 1981) which means that all objects must have the same opportunity of being included in the sample. The sampling paradigm that allows meeting the equal opportunity rule is called design-based sampling (Geuna, 2000). The term design refers to a system of sampling rules designed such that all objects in the sampling space have the same probability of being sampled. Design-based sampling can also be referred to as random sampling since its goal is to reach randomness.

Simple random sampling is the most basic random-based design and provides that all possible combinations of n sampling units have the same probability of being selected from among the total N sampling units in the population. However, this sampling approach requires a high amount of sampling to obtain a sufficient estimate precision and is impossible in histology as it would require the specimen to be glued together and resectioned after each section was selected (Geuna, 2000). Other random sampling designs include systematic, multistage, and stratified random sampling (Cochran, 1977). The most used approach in neuromorphology is systematic random sampling that is based on the systematic selection of every n^{th} unit of the population from one randomly selected starting unit (where n is the distance between units that is decided in relation to the amount of sampling required). In case of nerve fiber stereology, the units are the single sampling boxes on a given nerve cross section, and, after the starting box is selected by chance, the following boxes are selected by systematically jumping at a given distance from the former box (Fig. 5A).

Once the sampling fields are selected within the nerve cross section by systematic random sampling, it is necessary to define a set of inclusion/exclusion rules for clearly determining which nerve fiber falls inside the sampling field, and which other does not (Geuna et al., 2004). The bias originating from an unclear determination of inclusion/exclusion rules depends on the ‘‘edge effect’’ (Gundersen, 1977) that is due to variability in the size and morphology of fiber profiles which may cause significant differences in the probability of each profile being intersected by the frame edges: larger fibers will have a higher probability of intersecting the frame edges and thus of partially falling into more than one sampling field than smaller fibers. If all edging fiber profiles are excluded, quantitative estimations will be biased towards a systematic underestimation of number and size of fibers, while if all edging fiber profiles are included, quantitative estimations will be biased toward a systematic overestimation. In must be noted that many papers reporting data on nerve histomorphometry do not provide any information on ‘‘what happens’’ when a fiber profile intersects the histologic field edges.

To cope with the *edge effect*, the equal opportunity rule should be respected by adopting a set of inclusion/exclusion rules that assures that any fiber profile has the same chance of being sampled, irrespective of its morphological features. In other words, all fiber profiles must have the possibility of being selected in one histologic field only, irrespective of the number of edge intersections (Geuna et la., 2004). For nerve fiber quantitative assessment, two stereological methods have been the most employed so far for coping with the edge effect: the unbiased sampling frame (Gundersen, 1978; Larsen, 1998; Keskin et al., 2004; Acar et al., 2008; Canan et al., 2008) and the 2D disector (Gundersen, 1986; Geuna et al., 2000, 2001). We have specific experience with the latter methods that represents an adaptation of the disector principle (that is used for sampling object in 3D) and that it is basically an associated-point method, i.e. A method based on the identification of an “univocal” reference point in each particle (the “top”): the particle is then included in the sampling frame only if this point falls inside the frame independently from what happens to the rest of the particle (Geuna, 2000;2005). In the 2D disector, the “top” is identified as the “higher” edge of a fiber profile and thus nerve fibers are considered inside the frame, and thus counted; only when their “top” falls inside the sampling field borders (Fig. 5B). Whereas, the first description of the 2D-disector (Geuna et al., 2000) was based

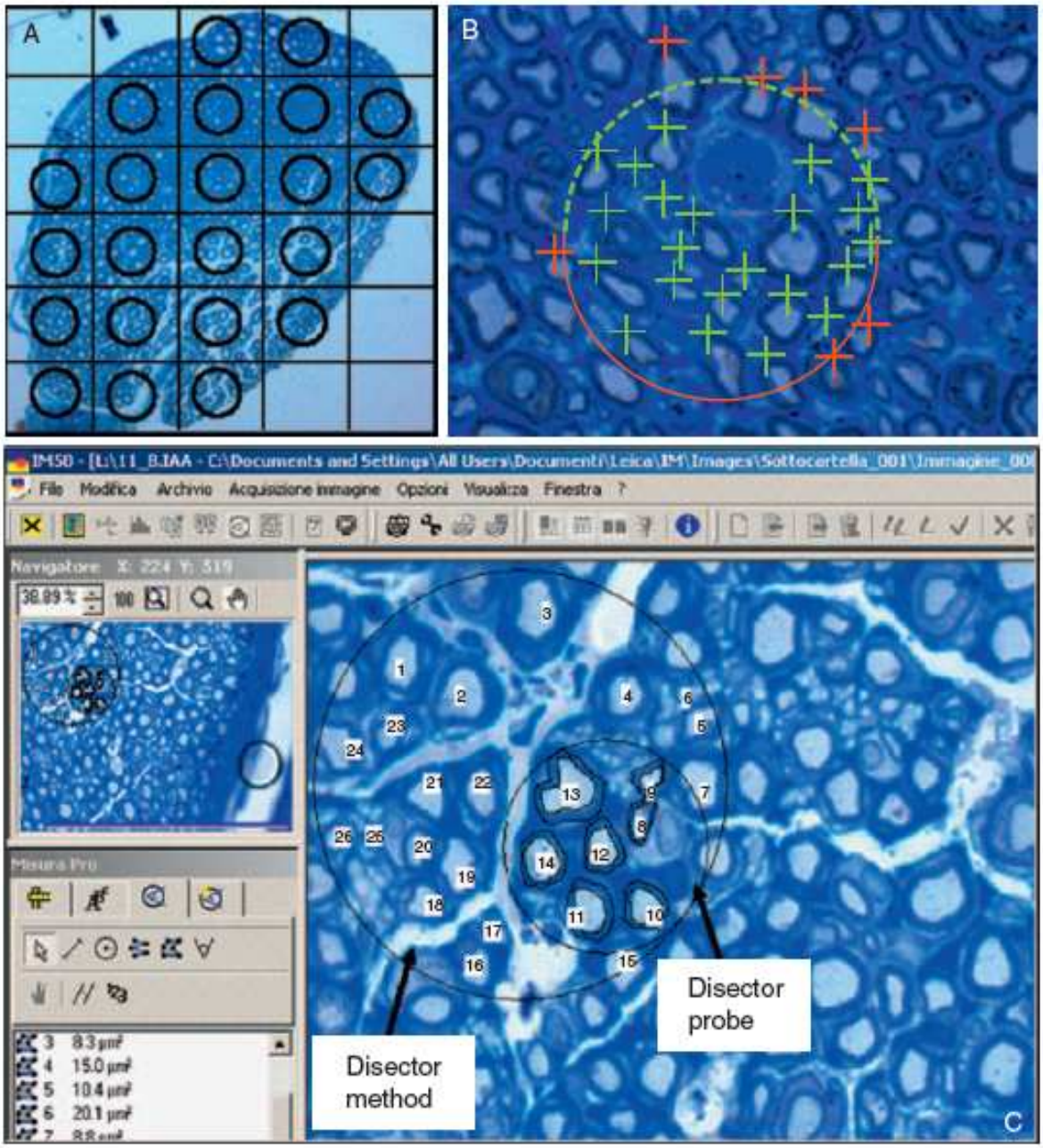

FIG. 5. (A) Systematic random sampling adapted for locating the sampling fields (the circles) all over the nerve profile. (B) Application of the 2D disector method for selecting fibers inside the circular sampling frame. Only fiber tops which fall inside the circle are selected. In case a fiber top falls exactly on the circle border an inclusion (green) and exclusion (red) half circle is preliminarily determined. (C) The selected fibers can be counted to estimate the total fiber number in that nerve (disector method). In the other case the disector is used as a probe to produce an unbiased sample of fibers respecting the equal opportunity rule (disector probe). Usually, the disector used as a probe is smaller than the disector for counting in order to avoid excessive workload in fiber measurement.

On the employment of a squared frame, we currently prefer to use a circular frame (Fig.5) in order to reduce the probability of nerve fibers (that have a circular shape) to hit the frame border. To make the decision also when a fiber's top exactly falls on the line, an inclusion hemi circle (the higher dashed green one) and an exclusion hemi circle (the lower red solid one in the example of Fig. 2B) can be identified and the fiber top is excluded from counting when it touches the lower hemi circle and vice versa.

From a practical viewpoint, in our laboratory we use a DM4000B microscope equipped with a DFC320 digital camera and an IM50 image manager system (Leica Microsystems, Wetzlar, Germany)(Fig.5C). This system reproduces microscopic images (for quantitative morphology of

myelinated nerve fibers, images should be captured through a 100x oil-immersion objective) on the computer monitor at a magnification adjusted by a digital zoom. The final magnification was 6,600x enabling accurate identification and morphometry analysis of myelinated nerve fibers. Figure 5C also shows the difference between the *disector (counting) method*, which allows obtaining an estimation of the number of objects, and the *disector probe* that allows selecting a random sample of objects for further carrying out measurements on them.

As most other authors, we carry out measurements just on one randomly selected section from each nerve. However, the use of a single section deserves mention since the quantitative parameters of nerve fibers can vary significantly depending on the nerve level and on the distance from the point of lesion (Santos, et al., 2007). Two methodological strategies can be adopted to avoid source of variability. The first and more laborious one is based on the calculation of mean values from data obtained on multiple sections taken at different levels of the nerve. A simpler alternative, is based on the use of a single section provided that a cutting procedure that assures that the section used for the quantitative assessment is taken at the same location along all nerves is adopted (e.g. 5mm distal to the site of lesion site in a nerve regeneration study). If adequate sampling techniques are employed (e.g. The 2-D disector), this approach provides unbiased data (Larsen, 1998; Geuna, et al., 2000).

Once the section is randomly selected, the total cross-sectional area of the nerve is measured and the sampling fields are then randomly selected using a simple procedure that we have described in details previously (Geuna, et al., 2000). Mean fiber density is then calculated by dividing the total number of nerve fibers within the sampling field by its area (N/mm^2). Total fibers number (N) is finally estimated by multiplying the mean fiber density by the total cross-sectional area of the whole nerve cross section.

Two-dimensional disector probes are then also used for the unbiased selection of a representative sample of myelinated nerve fibers in each of which both fiber and axon area are measured. From these two data, circle-fitting diameter of fiber (D) and axon (d) are calculated as well as myelin thickness [(D-d)/2], myelin thickness/axon diameter ratio [(D-d)/2d], and axon/fiber diameter ratio (d/D), the g-ratio (D/d).

Once a data set is obtained, the precision of the estimates is evaluated by calculating the coefficient of error (CE). Regarding quantitative estimates of fiber number, the *CE(n)* is obtained as follows: (Schmitz, 1998)

$$CE(n) = \frac{1}{\sqrt{\sum Q'}}$$

Where $\Sigma Q'$ is the number of counted fibers in all disectors.
For size estimates, the coefficient of error is estimated as: (Geuna, et al., 2001)

$$CE(z) = \frac{SEM}{Mean}$$

Where SEM = standard error of the mean.

The sampling scheme is usually designed in order to keep the CE below 0.10, which assures enough accuracy for neuromorphological studies (Pakkenberg and Gundersen, 1997).

Finally, numerical data are statistically analyzed by ANOVA. Statistical significance is established as $P < 0.05$. We perform statistical tests using the software “Statistica per discipline bio-mediche” (mcgraw-Hill, Milano, Italia).

V.1. Comparison of quantitative estimates between resin- and paraffin-embedded nerve specimens.

Although the gold standard for tissue processing is represented by toluidine blue staining of resin embedded semithin sections (Fig. 1F), we have recently described a simple protocol for pre-embedding staining of myelin sheath with osmium tetroxide on paraffin embedded sections (Fig. 1C) (Di Scipio et al., 2008). Pre-embedding osmium tetroxide fixation avoids myelin sheath swelling (Fig. 1C) and provides a sharp myelin staining that makes it possible the clear recognition of most myelinated nerve fibers and the measurement of their main quantitative parameters (axon and fiber diameter and myelin thickness) both on resin and paraffin-embedded specimens. This method represents a valid alternative to the conventional resin embedding-based protocol in comparison to which is much cheaper and can be carried out in any histological laboratory.

Since it has been shown that variable tissue shrinkage can occur due to embedding procedures (Ohnishi et al., 1974, Ward et al., 2008), a question arises regarding the possibility to directly compare quantitative data on myelinated nerve fibers obtained on nerve samples embedded in paraffin vs resin.

Therefore, we have carried out a comparative stereological analysis on paraffin- and resin-embedded rat radial nerves in order to verify whether the different embedding procedures might influence the quantitative estimates of size parameters of the myelinated axons. Four adult female Wistar rats, weighing approximately 250g, were used for the present study. Adequate measures were taken to minimize pain and discomfort taking into account human endpoints for animal suffering and distress. All procedures were performed with the approval of the Local Ethical Committee and in accordance with the European Communities Council Directive of 24 November 1986 (86/609/EEC). Under deep anesthesia by ketamine (40mg/250g) and cloropromazine (3.75mg/250g) and clean conditions, the left radial nerve was exposed at the middle third of the brachium and a 10-mm long segment withdrawn under operative microscope. Immediately after withdrawal, the nerve samples were divided into two segments of equally length. In order to facilitate the correct orientation for cutting, proximal specimen was marked by a 9-0 stitch on the proximal stump while in the distal specimen a 9-0 stitch was used to mark its distal stump.

The proximal specimens were fixed in 2.5% purified glutaraldehyde (Histo-line Laboratories s.r.l., Milano, Italy) and 0.5% saccarose in 0.1M Sorensen phosphate buffer, post-fixed in 2% osmium tetroxide and processed for resin embedding; the distal specimens were fixed in 4% paraformaldehyde (Fluka, Buchs, Switzerland) in PBS (Phosphate Buffered Saline), post-fixed in 2% osmium tetroxide and processed for paraffin embedding (see for detailed protocols: Di Scipio et al., 2008). From the resin-embedded proximal specimen, a series of ten 2-µm-thick sections was cut starting from its distal stump, while from the paraffin-embedded specimen a series of ten 8-µm-thick sections was cut starting from its proximal stump. In this way, all sections in each specimen were taken within a 100-µm-long radial nerve segment. Resin sections were finally stained by toluidine blue for 2 min while no counter-stain was used for paraffin sections since myelin fibers are easily recognizable.

Statistical analysis was performed using the one-way analysis of variance (ANOVA) test for comparing each parameter's mean values and the Wilcoxon Rank Sum non parametric test for comparions fiber size distribution. Statistical significance was established as $p < 0.05$.

Results of the statistical comparison showed that, when mean values are considered, no significant difference ($p>0.05$) was detected between resin-embedded and paraffin-embedded myelinated nerves (Table 1). On the other hand, when the Wilcoxon rank sum non parametric statistical analysis was applied to fiber diameter and myelin thickness distribution histograms (Fig. 6), significant ($p<0.05$) differences between the two types of tissue processing are observed.

VI. Conclusions

The experience of many years tell us that there is no single morphological technique which is intrinsically superior to the other and should thus be indicated as the gold standard for peripheral nerve regeneration research (Vleggeert-Lankamp 2007).

TABLE I

COMPARISON OF STEREOLOGICAL ESTIMATES OF MYELINATED NERVE FIBERS IN RESIN-EMBEDDED AND PARAFFIN-EMBEDDED NORMAL RAT RADIAL NERVES (VALUES ARE MEANS ± S.D)

	Resin-embedded	Paraffin-embedded
Total number of myelinated fibers	4041 ± 327	3898 ± 851
Density of fibers (#/mm^2)	11,541 ± 857	11,718 ± 3.287
Fibers diameter (μm)	7.80 ± 1.74	7.71 ± 0.93
Axons diameter (μm)	5.61 ± 0.73	5.52 ± 0.37
Myelin thickness (μm)	1.09 ± 0.51	1.10 ± 0.33
M/d	0.20 ± 0.06	0.21 ± 0.05
D/d	1.40 ± 0.12	1.42 ± 0.11
g-ratio	0.72 ± 0.06	0.71 ± 0.05

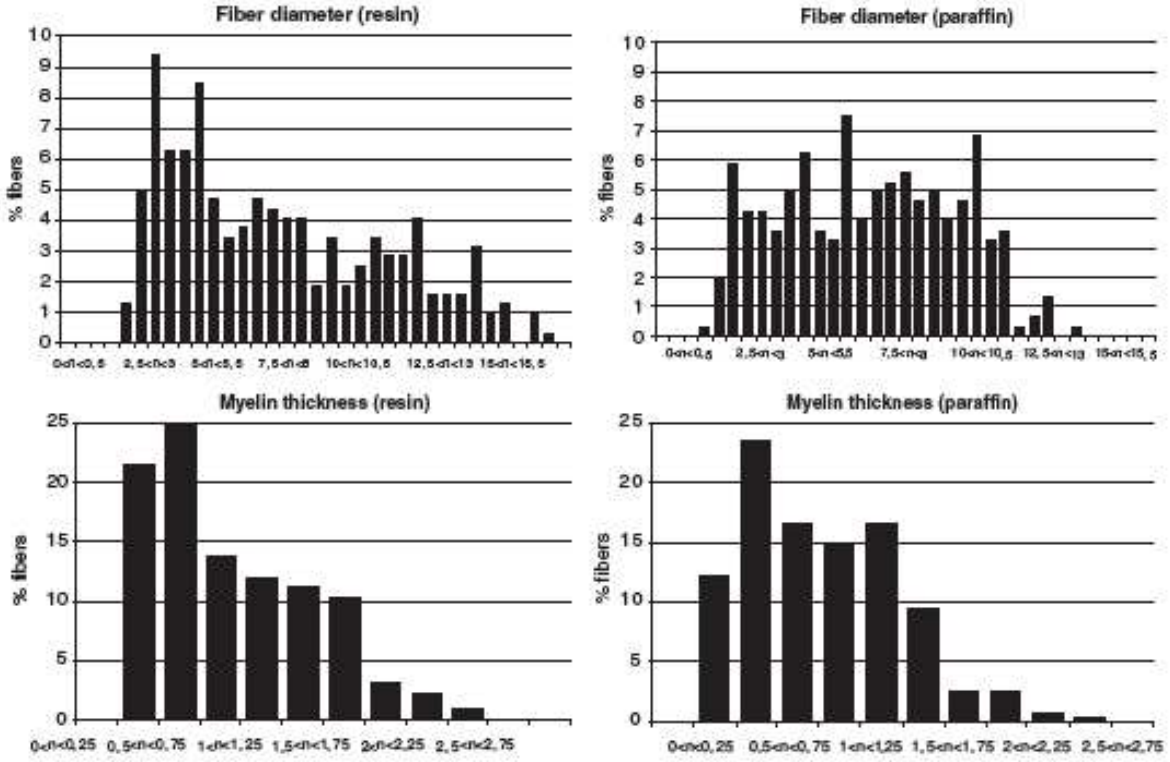

FIG. 6. Size distribution of fiber diameter and myelin thickness measurements comparing resin- and paraffin-embedded nerves. While mean values are not significantly different (Table I), nonparametric statistical analysis of size distribution ranks shows significant ($P < 0.05$) differences between the two types of embedding mediums.

On the other hand, the best methodology for histological assessment for any given study should be carefully selected on the basis of the study goals as well as of the available resources. Specifically, light microscopy should always be carried out and the simple introduction of osmium tetroxide pre-embedding staining can make light microscopy observation much more valuable independently from the embedding medium used (Di Scipio et al., 2008). Immunohistochemistry is a powerful technique which has a wide range of applications in peripheral nerve regeneration research both as a mean to mark and thus recognize the various elements of the nerve and as a tool for exploring the biological mechanism at a molecular level. Electron microscopy too is a powerful tool and, although its employment should be limited to selected research goals because of its high costs, this technique is particularly useful for investigating the early stages of nerve damage and regeneration at a subcellular level.

Histomorphometry is often the final step of morphological investigation since, to obtain an answer about any scientific question, a statistical comparison of numerical data between the different experimental groups must be sought. Although apparently simple, quantitative morphology is tricky and should be carried out carefully in order to avoid that bias creeps into the estimates (Geuna, 2000). Nowadays, stereology provides us a number of reliable methods for the quantitative assessment of peripheral nerve predictors during damage and regeneration. Original data reported in this paper suggest also that the direct comparison of quantitative results obtained from nerve specimens embedded in different mediums shall be evaluated carefully because of the influence of the embedding procedure on nerve fiber size distribution.

A final mention deserves the debate about the correlation between morphological and functional predictors of nerve regeneration. While it has been shown that some morphological parameters relate significantly with the functional predictor of nerve recovery (Kanaya et al., 1996; Prodanov and Feirabend, 2007), in most cases morpho-functional correlation is poor and thus the value of the combined use of both type of methodological approaches in nerve repair and regeneration research should be emphasized (Varejao et al., 2004; Castro et al., 2008; Geuna and Varejao, 2008).

6. References

Acar, M., Karacalar, A., Ayyildiz, M., Unal, B., Canan, S., Agar, E., and Kaplan, S. (2008). The effect of autogenous vein grafts on nerve repair with size discrepancy in rats: an electrophysiological and stereological analysis. *Brain Res.* **1198,** 171-181.

Audisio, C., Nicolino, S., Scevola, A., Tos, P., Geuna, S., Battiston, B., and Perroteau, I. (2008). Erbb receptors modulation in different types of peripheral nerve regeneration. *Neuroreport* **19**, 1605-1609.

Baryshnikova, L.M., Von Bohlen Und Halbach, O., Kaplan, S., and Von Bartheld, C.S. (2006). Two distinct events, section compression and loss of particles ("lost caps"), contribute to z-axis distortion and bias in optical disector counting. *Microsc. Res. Tech.* **69,** 738-756.

Benes, F.M., and Lange, N. (2001). Two-dimensional versus three-dimensional cell counting: a practical perspective. *Trends Neurosci.* **24,** 11-17.

Canan, S., Bozkurt, H.H., Acar, M., Vlamings, R., Aktas, A., Sahin, B., Temel, Y., and Kaplan, S. (2008). An efficient stereological sampling approach for quantitative assessment of nerve regeneration. *Neuropathol. Appl. Neurobiol.* **34,** 638-649.

Casha, S., Yong, V.W., and Midha, R. (2008). Minocycline for axonal regeneration after nerve injury: a double-edged sword. *Exp. Neurol.* **213,** 245-248.

Castro, J., Negredo, P., and Avendaño, C. (2008). Fiber composition of the rat sciatic nerve and its modification during regeneration through a sieve electrode. *Brain Res.***1190,** 65-77.

Cochran, W. G. (1977), Sampling Techniques, Third Edition, New York: John Wiley & Sons, Inc.

Coggeshall, R.E. (1992). A consideration of neural counting methods. *Trends Neurosci*. **15,** 9-13.

Cruz-Orive, L.M., and Weibel, E.R. (1981). Sampling designs for stereology. *J. Microsc.* **122,** 235-257.

Di Scipio, F., Raimondo, S., Tos, P., and Geuna, S. (2008). A simple protocol for paraffin-embedded myelin sheath staining with osmium tetroxide for light microscope observation. *Microsc. Res. Tech.* **71,** 497-502.

Fornaro, M., Geuna, S., Fasolo, A., and Giacobini-Robecchi, M.G. (2003). Huc/D confocal imaging points to olfactory migratory cells as the first cell population that expresses a post-mitotic neuronal phenotype in the chick embryo. *Neuroscience* **122,** 123-128.

Fornaro, M., Lee, J.M., Raimondo, S., Nicolino, S., Geuna, S., and Giacobini-Robecchi, M. (2008). Neuronal intermediate filament expression in rat dorsal root ganglia sensory neurons: an in vivo and in vitro study. *Neuroscience***153,** 1153-1163.

Fraher, J.P,. O'Leary, D., Moran, M.A., Cole, M., King, R.H., and Thomas, P.K. (1990). Relative growth and maturation of axon size and myelin thickness in the tibial nerve of the rat. 1. Normal animals. *Acta Neuropathol*. **79,** 364-374.

Geuna, S. (2005). The revolution of counting "tops": two decades of the disector principle in morphological research. *Microsc. Res. Tech.* **66,** 270-274.

Geuna, S., and Varejão, A.S. (2008). Evaluation methods in the assessment of peripheral nerve regeneration. *J. Neurosurg.* **109,** 360-362.

Geuna, S., Gigo-Benato, D., and Rodrigues Ade, C. (2004). On sampling and sampling errors in histomorphometry of peripheral nerve fibers. *Microsurgery* **24,** 72-76.

Geuna, S., Tos, P., Battiston, B., and Guglielmone, R. (2000). Verification of the two-dimensional disector, a method for the unbiased estimation of density and number of myelinated nerve fibers in peripheral nerves. *Ann. Anat.* **182,** 23-34.

Geuna, S., Tos, P., Guglielmone, R., Battiston, B., and Giacobini-Robecchi MG. (2001). Methodological issues in size estimation of myelinated nerve fibers in peripheral nerves. *Anat. Embryol.* **204,** 1-10.

Geuna, S., Raimondo, S., Ronchi, G., Di Scipio, F., Tos, P., and Fornaro, M. (2009). Histology of the peripheral nerve and changes occurring during nerve regeneration. *Int. Rev. Neurobiol.* This issue.

Gonzalez-Martinez, T., Perez-Piñera, P., Díaz-Esnal, B., and Vega, J.A. (2003). S-100 proteins in the human peripheral nervous system. *Microsc. Res. Tech.* **60,** 633-638.

Guillery, R.W. (2002). On counting and counting errors. *J. Comp. Neurol.* **447,** 1-7.

Gundersen, H.J.G. (1977). Notes on the estimation of the numerical density of arbitrary profiles: the edge effect. *J. Microsc.* **111,** 219-223.

Gundersen, H.J.G. (1978) Estimators of the number of objects per area unbiased by edge effects. *Microsc. Acta* **81,** 107-117.

Gundersen, H.J.G. (1986). Stereology of arbitrary particles. A review of unbiased number and size estimators and the presentation of some new ones, in memory of William R. Thompson. *J. Microsc.* **143,** 3-45.

Hall, S. (2005). The response to injury in the peripheral nervous system. *J. Bone Joint Surg.* **87,** 1309-1319.

Hoffman, E.O., Flores, T.R., Coover, J., and Garrett, II H.B. (1983). Polychrome stains for high resolution light microscopy. *Lab. Med.* **14,** 779-781.

Hoffman, P.N (1995) The synthesis, axonal transport, and phosphorilation of neurofilaments determine axonal caliber in myelinated nerve fibers. *Neuroscientist* **1,** 76–84

Inaga, S., Katsumoto, T., Tanaka, K., Kameie, T., Nakane, H., and Naguro, T. (2007). Platinum blue as an alternative to uranyl acetate for staining in transmission electron microscopy. *Arch. Histol. Cytol.* **70,** 43-49.

Kanaya, F., Firrell, J.C., and Breidenbach, W.C. (1996). Sciatic function index, nerve conduction tests, muscle contraction, and axon morphometry as indicators of regeneration. *Plast. Reconstr. Surg.* **98,** 1264-1271.

Keskin, M., Akbaş, H., Uysal, O.A., Canan, S., Ayyldz, M., Ağar, E., and Kaplan, S. (2004). Enhancement of nerve regeneration and orientation across a gap with a nerve graft within a vein conduit graft: a functional, stereological, and electrophysiological study. *Plast. Reconstr. Surg.* **113,** 1372-1379.

Larsen, J.O. (1998). Stereology of nerve cross sections. *J. Neurosci. Methods* **85,** 107-118.

Mayhew, T.M., and Gundersen, H.J (1996). If you assume, you can make an ass out of u and me': a decade of the disector for stereological counting of particles in 3D space. *J. Anat.* **188,** 1-15.

Onishi, A., Offord, K., and Dyck, P.J. (1974). Studies to improve fixation of human nerves. 1. Effect of duration of glutaraldehyde fixation on peripheral nerve morphometry. *J. Neurol. Sci.* **23,** 223-226.

Pakkenberg, B., and Gundersen HJ. (1997). Neocortical neuron number in humans: effect of sex and age. *J. Comp. Neurol.* **384,** 312-320.

Prodanov, D., and Feirabend, H.K (2007). Morphometric analysis of the fiber populations of the rat sciatic nerve, its spinal roots, and its major branches. *J. Comp. Neurol.* **503,** 85-100.

Reed, M.G., and Howard, C.V. (1998). Surface-weighted star volume: concept and estimation. *J. Microsc.* **190,** 350-356.

Santos, A.P., Suaid, C.A., Fazan, V.P., and Barreira, A.A. (2007). Microscopic anatomy of brachial plexus branches in Wistar rats. *Anat. Rec.* **290,** 477–485.

Schmitz, C. (1998). Variation of fractionator estimates and its prediction. *Anat. Embryol.* **198,** 371-397

Schmitz, C., and Hof, P.R. (2005). Design-based stereology in neuroscience. *Neuroscience* **130,** 813-831.

Varejão, A.S., Melo-Pinto, P., Meek, M.F., Filipe, V.M., and Bulas-Cruz, J. (2004). Methods for the experimental functional assessment of rat sciatic nerve regeneration. *Neurol. Res.* **26,** 186-194.

Vleggeert-Lankamp, C.L. (2007). The role of evaluation methods in the assessment of peripheral nerve regeneration through synthetic conduits: a systematic review. Laboratory investigation. *J. Neurosurg*. **107,** 1168-1189.

Von Bartheld, C. (2002). Counting particles in tissue sections: choices of methods and importance of calibration to minimize biases. *Histol. Histopathol.* **17,** 639-648.

Ward, T.S., Rosen, G.D., and von Bartheld, C.S. (2008). Optical disector counting in cryosections and vibratome sections underestimates particle numbers: effects of tissue quality. *Microsc. Res. Tech.* **71,** 60-88.

West, M.J. (1999). Stereological methods for estimating the total number of neurons and synapses: issues of precision and bias. *Trends Neurosci.* **22,** 51-61.